EDN: PJYJQI
УДК 537.9

Diffusion and Electromigration of Ions – Products of the Proton Exchange Reaction in a Benzoic Acid Melt

Vitaly A. Demin*
Maxim I. Petukhov†
Perm State University
Perm, Russian Federation

Received 10.08.2024, received in revised form 15.09.2024, accepted 24.10.2024

Abstract. The work is devoted to a numerical study of the transport of proton exchange reaction products in a benzoic acid melt after the interaction of its molecules with a lithium niobate crystal. Due to dissociative adsorption from the surface of the substrate, positive lithium ions and negative benzoate ions diffuse into the acid. The transfer of these reaction products is described using equations in the continuos media approximation. The mathematical model takes into account the diffusion and electromigration mechanisms of transport, as well as the recombination of ions. As a result of the solution, stationary distributions of ion concentrations are obtained. Due to the large difference in the kinetics of the reaction products, benzoate ions are grouped predominantly near the substrate, while lithium ions tend to move away from it to a much greater distance. The work shows that the size of the computational domain approaches the size of the reactor working space when the ions of both types form boundary layers.

Keywords: proton exchange, boundary layer, numerical simulation.

Citation: V.A. Demin, M.I. Petukhov, Diffusion and Electromigration of Ions – Products of the Proton Exchange Reaction in a Benzoic Acid Melt, J. Sib. Fed. Univ. Math. Phys., 2025, 18(1), 100–108. EDN: PJYJQI.

Introduction

The technology of enriching lithium niobate or lithium tantalate crystals with protons has been actively used in the manufacturing of waveguides over the past decades. This technology was first presented in the works [1, 2]. Its essence lies in the fact that a crystal sample is placed in a benzoic acid melt at characteristic temperatures ~ 500 K. As a result a complex chemical reaction occurs on the substrate surface. Dissociation of acid molecules after their interaction with the substrate leads to origin of negative benzoate ions and positive hydrogen ions on the crystal surface. Protons tend to penetrate the crystal and replace lithium ions, which diffuse from the near-surface region of the crystal into the acid. After some time, lithium ions recombine with the benzoate ions remaining in the acid. As a result the lithium benzoate molecules are formed. Thus, the protons penetrate into the crystal because of dissociative adsorption. As experiments show, protonation with duration $\sim 1-2$ h leads to the formation of a proton-enriched layer in the substrate with a thickness of $\sim 5-6$ μm.

Active implementation of this technology in the production of channel and planar waveguides has led to the emergence of a large number of its modifications [3]. Thus, to regulate the

*demin@psu.ru
†geniusmaxp@yandex.ru

protonation rate, impurities are used, added both to benzoic acid [4, 5] and to the crystal [6] before protonation. The presence of protons in the crystal changes its refractive index. Numerous experiments show that the refractive index profiles, as well as the proton concentration profiles in the formed near-surface layer of the crystal, have a characteristic stepped shape [1, 7]. These profiles can be smoothed by additional annealing after proton exchange [8]. Many works are devoted to the study of the complex phase structure of the crystal after its enrichment with protons [9] and the effect of the conditions of proton exchange on this structure. For example, the surfaces of samples are subjected to preliminary plasma treatment [10]. At present, special attention is paid to the protonation of thin-film lithium niobate [11, 12].

Theoretical investigation of the protonation process began with the work of Vohra [7], devoted to the study of hydrogen ion transport inside the crystal. The results of this work demonstrated a strong influence of the ion flux nonlinearity in the transport equation during description the process of lithium ion substitution by protons. In turn, the annealing process is described using the classical diffusion equation.

According to other works, the diffusion of lithium ions and benzoate ions into the benzoic acid melt during protonation leads to the formation of a stationary boundary layer by benzoate ions [13, 14]. This investigation shows that the transport and subsequent recombination of the reaction products can be described using equations in the continuous media approximation. Most of the lithium benzoate is produced in thin near-surface layer in the melt. It is known from experiments that the presence of this impurity reduces the intensity of proton exchange even at a small content of lithium benzoate in the melt [5]. Clarification of the characteristics of the resulting boundary layer allows us to understand possible methods for controlling the proton exchange process.

In the mentioned work [14] the size of the computational domain was comparable with the thickness of the photolithographic mask ($\sim$ 2 μm), which, on the one hand, is sufficient to qualitatively show the presence of the boundary layer, but, on the other hand, can greatly underestimate its size. Lithium ions, having a mobility an order of magnitude greater than benzoate ions, are capable of moving away from the protonated surface. Then lithium ions reach the opposite impenetrable boundary of the computational domain and, due to more intensive recombination, prevent the diffusion of benzoate ions deep into the melt. This circumstance is the reason why the transport of reaction products must be considered in regions which size is much larger than the characteristic thickness of the photolithographic mask.

In the work [15] an asymptotic solution is obtained, which allows to estimate the thickness of the boundary layer in the case when the size of the region under consideration are comparable with the size of the reactor in which the proton exchange takes place. It should be noted that, despite more realistic problem geometry, in this work a strong assumption is made. It consist in neglecting the influence of the electric field formed in the region occupied by ions on their concentration profiles. Because of this, according to the obtained analytical solution, the thickness of the boundary layer grows indefinitely with the size of the reactor according to a power law.

In this paper, a more complete mathematical formulation is considered in order to obtain realistic characteristics of the boundary layer formed by ions.

1. Formulation of the problem

Let us consider a benzoic acid melt in contact with a homogeneous surface of a lithium niobate crystal. The temperature of this melt is assumed to be constant and equal to 500 K, which is

sufficient for proton exchange. Thus, lithium ions and benzoate ions should diffuse the melt from the crystal side. Diffusion, electromigration, and recombination of ions are described using the following system of equations in the continuous media approximation [16–18]:

$$\operatorname{div}(\varepsilon_0 \varepsilon \boldsymbol{E}) = e(n_+ - n_-), \qquad \boldsymbol{E} = -\nabla\varphi, \tag{1}$$

$$\frac{\partial n_\pm}{\partial t} = D_\pm \Delta n_\pm \mp \nabla(k_\pm n_\pm \boldsymbol{E}) - k_R n_+ n_-, \tag{2}$$

where $\boldsymbol{E}$, φ, $n_\pm$ are the fields of electric field strength, electric potential, and concentrations of positive and negative ions. Concentration determines the number of ions per unit volume and has a unit of measurement of m^{-3}. Parameters e, ε, ε_0 are the electron charge, the permittivity of benzoic acid, and the electric constant. The diffusion coefficients, the mobility of lithium and benzoate ions, and the recombination coefficient are denoted, correspondingly, by $D_\pm$, $k_\pm$, and k_R.

The coefficient of ion mobility relates the speed of their drift in the melt to the intensity of the external electric field [19]. The estimation of diffusion and ion mobility coefficients for the conditions of the present problem, as well as the comparison of these values with known experimental data, were carried out in accordance with [13, 19, 20].

According to the results obtained in [14], in the formulation under consideration there are no conditions for convective mass transfer [21], which allows us to describe the ion transport in a one-dimensional formulation. After eliminating the electric field strength, the system of equations (1)–(2) will have the form:

$$\varepsilon_0 \varepsilon \varphi'' = e(n_- - n_+), \tag{3}$$

$$\frac{\partial n_\pm}{\partial t} = D_\pm n_\pm'' \pm k_\pm (n_\pm' \varphi' + n_\pm \varphi'') - k_R n_+ n_-. \tag{4}$$

The prime denotes the derivative with respect to the x coordinate. The coordinate axis is directed along the normal to the crystal toward the melt. The interphase boundary is being considered as the origin of coordinates. The boundary conditions on it relate the derivative of the concentration to the ion flux density J, and also determine the reference point for the electric potential:

$$x = 0: \qquad n_\pm' = -\frac{J}{D_\pm}, \qquad \varphi = 0. \tag{5}$$

At a distance h from the crystal, an impenetrable reactor wall is modeled, on which, in addition, there is no electric field:

$$x = h: \qquad n_\pm' = 0, \qquad \varphi' = 0. \tag{6}$$

The combination of boundary conditions (5)–(6) ensures the electrical neutrality of the system:

$$\int_0^h n_+ dx = \int_0^h n_- dx. \tag{7}$$

The boundary value problem (3)–(7) was solved in dimensionless variables. The units of length, time, concentration and electric potential were taken to be h, h^2/D_+, Jh/D_+ and $eJh^3/\varepsilon_0\varepsilon D_+$, correspondingly. In these variables, the system of equations and boundary conditions are written in the following form:

$$\varphi'' = n_- - n_+, \tag{8}$$

$$\frac{\partial n_\pm}{\partial t} = A_\pm n''_\pm \pm B_\pm (n'_\pm \varphi' + n_\pm \varphi'') - C n_+ n_-, \tag{9}$$

$$x = 0: \qquad n'_\pm = -\frac{D_+}{D_\pm}, \qquad \varphi = 0, \tag{10}$$

$$x = 1: \qquad n'_\pm = 0, \qquad \varphi' = 0, \tag{11}$$

where

$$A_\pm = \frac{D_\pm}{D_+}, \qquad B_\pm = \frac{k_\pm e J h^3}{D_+^2 \varepsilon_0 \varepsilon}, \qquad C = \frac{k_R J h^3}{D_+^2}. \tag{12}$$

When varying the dielectric constant, it is taken into account that the recombination coefficient also changes with it [17]:

$$k_R = \frac{e(k_+ + k_-)}{\varepsilon_0 \varepsilon}. \tag{13}$$

2. Solution technique

To solve the boundary value problem (8)–(11), an explicit finite-difference scheme was used, implemented using a program written in the C++ programming language. The Poisson equation (8) was solved using the Liebman [22] scheme. Zero concentration and electric potential fields were used as initial conditions: $n_\pm(t = 0, x) = \varphi(t = 0, x) = 0$. The following values of dimensional parameters were used in the calculations: $k_+ = 1.5 \cdot 10^{-7}$ m^2/s·V, $k_- = 2 \cdot 10^{-8}$ m^2/s·V, $D_+ = 10^{-8}$ m^2/s, $D_- = 10^{-9}$ m^2/s, $J = 10^{18}$ s^{-1}m^{-2}. The value of the permittivity ε varied in the range from 1 to 20 [14]. In turn, the sizes of the computational domain h were taken in the range from $2 \cdot 10^{-6}$ to 10^{-4} m.

Based on the results obtained earlier in [15], equations (4) have an analytical solution in the case when $k_\pm = 0$. Using the multiple scales method, we can determine the boundary layer thickness δ, which is represented in the following form:

$$\delta = \frac{5 h^{\frac{1}{4}}}{\left(\frac{k_R J}{D_-}\left(\frac{1}{D_-} - \frac{1}{D_+}\right)\right)^{\frac{1}{4}}}. \tag{14}$$

It follows from this formula that for the values of h used in the present calculations the size of the boundary layer will be 1–2 orders of magnitude smaller than the size of the computational domain. In order to minimize the numerical errors that potentially arise in the thin region occupied by the boundary layer, and at the same time to save computer time, it is necessary to thicken the computational grid near the origin.

The grid thickening was carried out according to the many-stage scheme. After determine the size of the computational domain h, a uniform grid was formed, the nodes of which were located at points with coordinates x_i. Then, the variable step h_i was calculated for a non-uniform grid with the same number of nodes:

$$h_i = a + b x_i^c. \tag{15}$$

Thus, the computational domain was divided into 201 computational nodes, with a step of h_i. The values of the coefficients a, b and index c were selected in such a way that there were at least 100 nodes per ion boundary layer. The specificity of distribution (15) allows the grid nodes to be thickened in such a way that the grid step in the region occupied by the boundary layer is constant. An example of grid step distribution is shown in Fig. 1a.

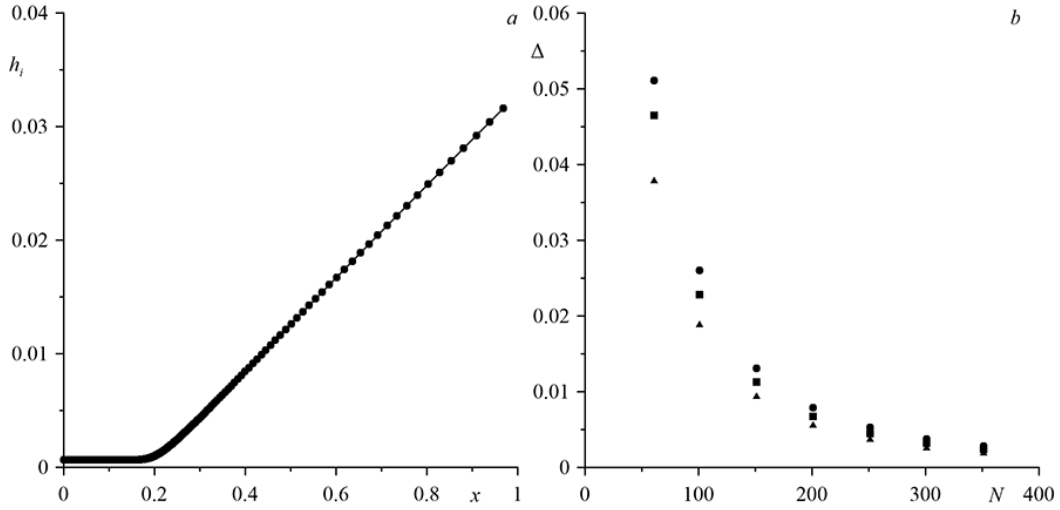

Fig. 1. Example of grid step distribution depending on coordinate for $a = 0.1$, $b = 5$, $c = 16$ (a); relative error Δ of the boundary layer thickness calculation (triangles) and the concentration of positive and negative ions in the center of the computational domain (circles and squares, correspondingly) depending on the number of nodes N (b)

When representing the system of equations (8)–(9) in finite difference form, the partial derivatives with respect to the coordinate x were calculated as follows:

$$\frac{\partial u}{\partial x} = \frac{u_{i+1} - u_{i-1}}{h_i + h_{i+1}}, \tag{16}$$

$$\frac{\partial^2 u}{\partial x^2} = \frac{2}{h_i + h_{i+1}} \left(\frac{u_{i+1} - u_i}{h_{i+1}} - \frac{u_i - u_{i-1}}{h_i} \right). \tag{17}$$

When calculating the spatial derivatives in the boundary conditions of the second kind (10)–(11), as well as the time derivative in equations (9), a one-sided difference was used:

$$\frac{\partial u}{\partial \tilde{x}} = \frac{u_{i+1} - u_i}{\tilde{h}}, \tag{18}$$

where $\tilde{x}$ is a generalized designation of the differentiation variable. In turn, $\tilde{h}$ is a generalized designation of the step along the coordinate at the side points of the computational domain, as well as the time step. An example of the convergence of the implemented scheme is shown in Fig. 1b. Expressions (16)–(18) are first-order formulas.

3. Results of numerical simulation

Solution of the boundary problem (8)–(11) gives stationary profiles of concentration and electric potential in the benzoic acid melt. Their characteristic form is shown in Fig. 2. The time necessary to originate stationary profiles in the model case, when the only ion transport mechanism is diffusion, is ~ 0.02 s. In turn, the reverse effect of the electric field on the concentration profiles additionally stabilizes the system and reduces this time up to ~ 0.01 s. It should be noted that in this case the process of stationary profiles origination is longer compared to one discussed in [14], since the size of the computational domain is significantly larger.

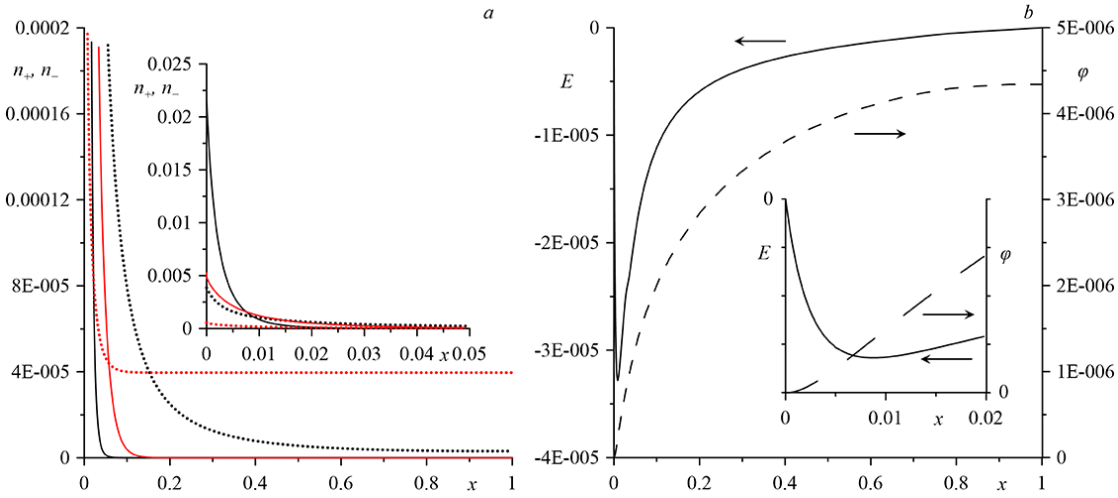

Fig. 2. Profiles of concentration (a), field strength and electric potential (b) at $h = 8 \cdot 10^{-5}$ m and $\varepsilon = 10$. Black and red curves correspond to the cases with and without electromigration, correspondingly. a) Solid lines — concentration of benzoate ions, dots — concentration of lithium ions. b) Solid lines — electric field strength, dashed lines — electric potential

Depending on whether electromigration is taken into account or not, a fundamental difference in the profiles is noticeable from Fig. 2a. In the purely diffusion case ($k_\pm = 0$), lithium ions reach the opposite boundary one way or another by the time of stationary profiles origination. These ions are present everywhere in the calculation region albeit in small concentrations. Including electromigration in the model allows the electric field formed, the strength of which is directed toward the crystal, to affect the ions. Thus, the lithium ion profile is slightly "pressed" to the interphase boundary. As calculations have shown, in the case of large h, the concentration of positive ions reaching the reactor wall tends to zero. Thus, concentration profile of these ions is qualitatively no different from the concentration profile of benzoate ions.

Having significantly lower mobility than lithium ions, benzoate ions are not able to reach the reactor wall in any case. These ions always form a boundary layer, the thickness of which varies depending on how far the lithium ions can move away from the interface. In other words, taking into account electromigration in the case where the size of the computational domain is large enough leads to the formation of a coupled boundary layer.

Fig. 2b shows the profiles of the electric potential and electric field strength. Comparing these profiles with the concentration profiles, it is easy to see that the electric field is most intense in the region of the benzoate ion boundary layer. The strength locally reaches $3 \cdot 10^4$ V/m. The electric field strength on the crystal surface is considered to be zero. This should be true in the case where the X-cut of lithium niobate is protonated. Despite the fact that the condition on the potential (5) is set at the crystal-melt boundary (but not on its derivative), the zero value of the strength is obtained in the solution process.

The characteristic thickness of the benzoate ion boundary layer depending on the size of the domain is shown in Fig. 3. It is evident that the results of solving the diffusion-recombination problem qualitatively repeat the analytical solution [15] and the layer thickness grows indefinitely with increasing h. In turn, electromigration does not allow lithium ions to move away from the crystal at an arbitrarily large distance, therefore, at a certain value of $h^* \approx 2 \cdot 10^{-5}$ m, they form

a boundary layer. At $h > h^*$, the characteristics of the boundary layers remain the same as in the case of $h = h^*$. According to this result one can say that h^* corresponds to Debye length of the investigated system.

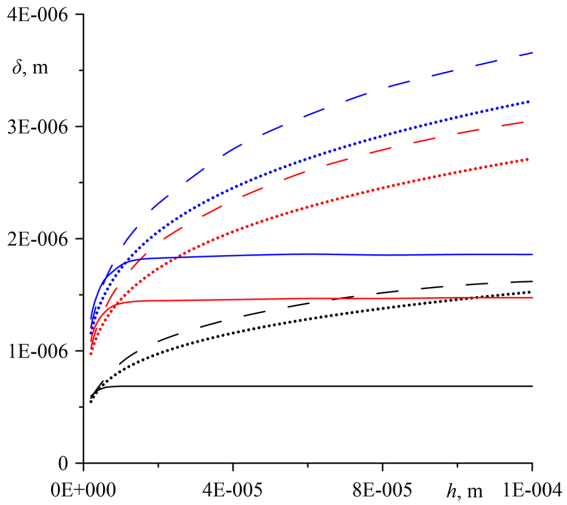

Fig. 3. Dimensional values of boundary layer thickness for the case of different permittivities. Dots and dashed lines are the results of analytical [15] and numerical solutions for $k_{\pm} = 0$; solid lines are the numerical solution with account of electromigration. Black, red and blue curves correspond to the case of $\varepsilon = 1$, 10 and 20, correspondingly

It is interesting to note that the effect of the electric field on the concentration profiles not only "presses" the positive lithium ion profiles toward the crystal, but also reduces the size of the region in which negative benzoate ions are present. The primary cause of this effect is a more intense recombination associated with an increase in the concentration of lithium ions affected by the electric field in the region near the crystal occupied by benzoate ions. Since the flux density of positive and negative ions from the crystal surface is the same, the total number of ions present in the melt should decrease, causing the boundary layer to shift toward the crystal.

Conclusion

As calculations have shown, after diffusion of lithium ions and benzoate ions into the benzoic acid melt, ion transport complicated by electromigration and recombination takes place. Due to the large difference in the kinetics of negative and positive ions participating in the proton exchange, the concentration profiles differ considerably from each other and an electric field is formed near the interphase. Taking into account the reverse effect of this field on ions greatly changes the concentration profiles in the case when the size of the computational domain exceed $2 \cdot 10^{-5}$ m. Analysis of the behavior of ions in a cavity with sufficiently large sizes allows us to establish that not only benzoate ions, but also lithium ions form a stationary boundary layer. The sizes of these structures remain unchanged with further growth of the computational domain and are $2 \cdot 10^{-6}$ m for benzoate ions and $2 \cdot 10^{-5}$ m for lithium ions, correspondingly.

The work was supported by the Russian Science Foundation (Grant No. 24-29-20277) and Perm Region.

References

[1] J.L.Jackel, C.E.Rice, J.J.Veselka, Proton exchange for high-index waveguides in $LiNbO_3$, *Appl. Phys. Lett.*, **41**(1982), 607–608.

[2] J.L.Jackel, Proton exchange: past, present, and future, *Proc. SPIE*, **1583**(1991), 54–63.

[3] M.Kuneva, Optical waveguides obtained via proton exchange technology in $LiNbO_3$ and $LiTaO_3$ – a short review, *International Journal of Scientific Research in Science and Technology*, **2**(2016), 40–50.

[4] S.S.Mushinsky, A.M.Minkin, I.V.Petukhov et al., Water Effect on Proton Exchange of X-cut Lithium Niobate in the Melt of Benzoic Acid, *Ferroelectrics*, **476**(2015), 84–93. DOI: 10.1080/00150193.2015.998530

[5] V.I.Kichigin, I.V.Petukhov et al., Structure and properties of proton exchange waveguides on Z cut of lithium niobate crystal fabricated in molten benzoic acid with the addition of lithium benzoate, International Conference and Seminar of Young Specialists on Micro/Nanotechnologies and Electron Devices, 2012, 238–241.

[6] A.V.Sosunov, S.S.Mushinsky et al., Evalua-tion of applicability of lithium niobate crystals Z-cut with predetermined impurity distribution for manufacturing of proton-exchanged waveguides, *Bulletin of Perm University. Physics*, **2**(2017), 69–73. DOI: 10.17072/1994-3598-2017-2-69-74

[7] S.T.Vohra, A.R.Mickelson, S.E.Asher, Diffusion characteristics and waveguiding properties of proton-exchanged and annealed $LiNbO_3$ channel waveguides, *J. Appl. Phys.*, **66**(1989), 5161–5174. DOI: 10.1063/1.343751

[8] M.De Micheli, J.Botineau, S.Neveu, P.Sibillot, D.B.Ostrowsky, Independent control of index and profiles in proton-exchanged lithium niobate guides, *Optics Lett.*, **8**(1983), 114–115. DOI: 10.1364/ol.8.000114

[9] Yu.N.Korkishko, V.A.Fedorov, Structural phase diagram of $H_xLi_{1-x}NbO_3$ waveguides: the correlation between optical and structural properties, *IEEE J. Sel. Top. Quantum Electron*, **2**(1996), 187–196. DOI: 10.1109/2944.577359

[10] I.V.Petukhov, V.I.Kichigin, S.S.Mushinskii, D.I.Sidorov, O.R.Semenova, The influence of plasma treatment of lithium niobate crystal surface on the proton exchange process in molten benzoic acid, *Bulletin of Perm University. Chemistry*, **9**(2019), 371-379. DOI: 10.17072/2223-1838-2019-4-371-379

[11] A.A.Kozlov, U.O.Salgaeva, V.A.Zhuravlev, A.B.Volyntsev, The study of the kinetics of thin-film lithium niobate reactive ion etching in a fluorine-containing plasma, *Bulletin of Perm University. Physics*, **1**(2024), 56–71.

[12] Y.Li, T.Lan, D.Yang, Z.Wang, Fabrication of ridge optical waveguide in thin film lithium niobate by proton exchange and wet etching, *Optical Materials*, **120**(2021), 111433. DOI: 10.1016/j.optmat.2021.111433

[13] V.A.Demin, M.I.Petukhov, R.S.Ponomarev, An ionic boundary layer near the lithium niobate surface in the proton exchange process, *Surface Engineering and Applied Electrochemistry*, **59**(2023), 321–328. DOI: 10.3103/S1068375523030055

[14] V.A.Demin, M.I.Petukhov, R.S.Ponomarev, M.Kuneva, Effect of Permittivity on the Ionic Boundary Layer upon Protonation of Lithium Niobate, *Journal of Siberian Federal University. Mathematics and Physics*, **16(5)**(2023), 611–619. EDN: GVVEKJ

[15] V.A.Demin, M.I.Petukhov, Application of multiple scales method to the problem about characteristics of the ionic layer near the surface of lithium niobate crystal in a benzoic acid melt, *Microgravity Science and Technology*, **36, 33**(2024). DOI: 10.1007/s12217-024-10113-z

[16] L.D. Landau, E.M. Lifshitz, Fluid Mechanics, Vol 6, Butterworth-Heinemann, 1987.

[17] F.Pontiga, A.Castellanos, Physical mechanisms of instability in a liquid layer subjected to an electric field and a thermal gradient, *Phys. Fluids*, **6**(1994), 1684.

[18] E.A.Demekhin, N.V.Nikitin, V.S.Shelistov, Direct numerical simulation of electrokinetic instability and transition to chaotic motion, *Phys. Fluids*, **25**(2013), 122001. DOI: 10.1063/1.4843095

[19] G.I.Skanavi, Fizika dielektrikov. Oblast' slabyh polej, *Moskva, Gosudarstvennoe izdatel'stvo tekhniko-teoreticheskoj literatury*, 1949 (in Russian).

[20] I.K.Kikoin, Tablicy fizicheskih velichin, Moskva, Atomizdat, 1976) (in Russian).

[21] G.Z.Gershuni, E.M.Zhukhovitskii, Convective stability of incompressible fluids, Jerusalem, Keter Publishing House, 1976.

[22] P.Roache, Computational fluid dynamics, Albuquerque, Hermosa publishers, 1976.

Диффузия и электромиграция ионов – продуктов реакции протонного обмена в расплаве бензойной кислоты

Виталий А. Демин
Максим И. Петухов
Пермский государственный университет
Пермь, Российская Федерация

Аннотация. Работа посвящена численному исследованию транспорта продуктов реакции протонного обмена в расплаве бензойной кислоты после взаимодействия ее молекул с кристаллом ниобата лития. Вследствие диссоциативной адсорбции с поверхности подложки в кислоту проникают положительные ионы лития и отрицательные бензоат-ионы. Перенос данных продуктов рекции описывается при помощи уравнений в приближении сплошной среды. В математической модели учитываются диффузионный и электромиграционный механизмы транспорта, а также рекомбинация ионов. В результате решения получаются стационарные распределения концентрации ионов. Из-за большой разницы в кинетике продуктов реакции бензоат-ионы группируются преимущественно вблизи подложки, в то время как ионы лития стремятся отдалиться от нее на гораздо большее расстояние. В работе показано, что при устремлении размеров расчетной области к размерам рабочего пространства реактора, ионы обоих типов формируют пограничные слои.

Ключевые слова: протонный обмен, пограничный слой, численное моделирование.